Overexposure Correction using Optimization-Based Multiple Cylinder Fitting in CT

Alexander Preuhs[1],Martin Berger[1,2], Yan Xia[1,3], Andreas Maier[1], Joachim Hornegger[1], Rebecca Fahrig[4]

[1]Pattern Recognition Lab, FAU Erlangen-Nürnberg
[2]Research Training Group 1773 "Heterogeneous Image Systems"
[3]Erlangen Graduate School in Advanced Optical Technologies (SAOT)
[4]Department of Radiology, Stanford University, Stanford, CA, USA
alexander.preuhs@fau.de

Abstract. Flat-Panel Computed Tomography (CT) has found its commonly used applications in the healthcare field by providing an approach of examining 3D structural information of a human's body. The popular CT reconstruction algorithms are based on a filtered backprojection (FBP) scheme, which would face challenges when imaging the knee. This is because in some views, the X-rays are highly attenuated when traveling through both thigh bones. In the same view, X-rays also travel through soft tissue that absorbs much less energy with respect to bone. When these high intensity X-rays arrive at the detector they cause detector saturation and the generated sinogram suffers from overexposure. Reconstructing an overexposed sinogram results in images with streaking and cupping artifacts, which are unusable for diagnostics. In this paper, we propose a method to correct overexposure artifacts using an optimization approach. Parameters describing a specific geometry are determined by the optimization and then used to extrapolate the overexposed acquisition data.

1 Introduction

In X-ray imaging, overexposure typically refers to a situation where the intensity range of the traveled X-rays in projections are greater than the detector's inherent detectable range — that is a dynamic range of 14 Bit . In Flat-Panel CT these circumstances can arise when examining the knee and are amplified by an automatic tube current and voltage modulation.

The overexposure occurs in views where the X-rays travel through both femurs (thigh bones). Then certain X-rays are attenuated strongly by two thigh bones, while other X-rays are attenuated less by soft tissue. The resulting amplitude range of the incoming X-rays is greater then the detectable range of the detector. The pixels that measure the less attenuating soft tissue receive numerous X-ray photons which causes saturation. In these locations not all the data

can be collected and the sinogram suffers from discontinuity between measured and unmeasured data.

In the sense of the resulting discontinuity, the overexposure problem is similar to a truncation occurring from an object extending the field of view. The high-pass-filtering during the FBP algorithms intensifies discontinuities and leads to cupping artifacts in the reconstructed image. In this manner, approaches concerning truncation correction can thus be used to correct overexposure artifacts.

That is often done by extrapolating the missing data, using an estimation model. Hsieh et al. [1] fit a water cylinder at the transitions between the measured- and unavailable data and use a mass constraint to post-fit them. Instead of water cylinders Ohnesorge et al. [2] use the mirrored values of the available data to extrapolate the missing areas. Ritschl et al. [3] use an additional low intensity scan for extrapolation. Gompel et al. [4] correct the discontinuity by fitting a single ellipse in the projections using consistency conditions as constraints. An implicit extrapolation scheme in the derivative domain was also investigated recently [5], [6].

In the proposed method, the missing data is extrapolated using multiple cylinder shapes that are fitted in the sinogram domain. The parameters describing these objects are estimated from the overexposed data using an optimization-based approach, by minimizing the least square error. This differs from the optimization approach proposed by Maier et al. [7], in which a water-cylinder was used to initialize the optimization but the objective function concentrates on high frequency artifacts and constant extrapolation in the reconstruction domain.

2 Materials and Methods

2.1 Two-Dimensional Imaging Geometry

The Radon transform of a 2D object function $f(x, y)$ in parallel-beam geometry is defined as

$$p(s,\theta) = \int_{-\infty}^{\infty}\int_{-\infty}^{\infty} f(x,y)\delta(x\cos\theta + y\sin\theta - s)\mathrm{d}x\mathrm{d}y \ , \tag{1}$$

where s is the distance from the central ray and θ defines the view angle of the system. By introducing a fan-angle γ and the view angle of a fan-beam system β, the equation can be expressed in fan-beam geometry by

$$p(s,\theta) = p(\gamma,\beta) \qquad \forall\theta \in \Theta \wedge \forall s \in S \ , \tag{2}$$

with $\Theta = \{\theta \mid \theta = \beta + \gamma\}$ and $S = \{s \mid s = D\sin\gamma\}$, where D defines the focal length.

2.2 Optimization-Based Multiple Shape Fitting

By its simple and smooth geometric properties, cylinder shapes are fitted in the sinogram domain. The forward transformation to the sinogram domain is given

by equation (1). We use that equation and insert for $f(x, y)$ the formulation of a cylinder with radius r that has the density ρ inside the region $x^2 + y^2 \leq r^2$. The resulting integration along a ray leads to a multiplication of the intersection length with the density of the cylinder positioned at the intersection. With the distance s between any ray and the central ray together with the radius of the cylinder r, the projection can be gained using simple trigonometry

$$p(s, \theta) = 2\rho\sqrt{r^2 - s^2} \ . \tag{3}$$

Equation (3) is defined in parallel-beam geometry. To convert the equation to the fan-beam geometry and a general off centered case, with the new center coordinates (c_x, c_y), we substitute the distance parameter s with $(D \sin\gamma - c_x \sin\theta - c_y \cos\theta)$ constrained by $(\theta = \beta + \gamma)$, thus

$$p_{\text{cyl}}(c_x, c_y, r, \rho, \gamma, \beta) = 2\rho\sqrt{r^2 - (D \sin\gamma - c_x \sin\theta - c_y \cos\theta)^2} \ . \tag{4}$$

Equation (4) provides the projection value of a cylinder along any ray defined by γ and β in fan-beam geometry. Defining a single cylinder with respect to its parameters and with the Radon transform providing the property of linearity, the projection resulting from a composition of cylinders is a summation. It can be calculated by

$$p(\gamma, \beta) = \sum_i p_{\text{cyl}}(c_{x_i}, c_{y_i}, r_i, \rho_i, \gamma, \beta) \ . \tag{5}$$

In the proposed method, the knee should be approximated as a composition of cylinders. The goal is to extrapolate the overexposed areas with forward projections of fitted cylinders. Therefore, we minimize the difference between the projections of a set of fitted cylinders $\sum_i p_{\text{cyl}}(c_{x_i}, c_{y_i}, r_i, \rho_i, \gamma, \beta)$ and the measured data $p_{\text{meas}}(\gamma, \beta)$. The parameters describing cylinders are optimized, so that the least-squares are as small as possible over the available data. That gives the objective function

$$\underset{\sum_{i=1}^{N} c_{x_i}, c_{y_i}, r_i, \rho_i}{\operatorname{argmin}} \sum_{\gamma \in \Omega} \sum_{\beta \in \Omega} \left| p_{\text{meas}}(\gamma, \beta) - \sum_{i=1}^{N} p_{\text{cyl}}(c_{x_i}, c_{y_i}, r_i, \rho_i, \gamma, \beta) \right|_2^2 \ . \tag{6}$$

The set Ω includes all the parameter pairs (γ, β) that correspond to data that does not suffer from overexposure. It can be determined prior to the reconstruction by simple thresholding of the raw detector values.

Also note that any other geometric object desired can be plugged into the objective function, if an analytic formulation of its Radon transform is available.

2.3 Experimental Setup

The used synthetic knee phantoms are a composition of cylindrical and elliptical shapes which are shown in Figure 1(a) and 1(e), respectively. The two thigh bones are represented by two cylinders having the density of bones. The two

knee caps (patellas) are simulated using two ellipses with the same density. The phantoms differ in the representation of the soft tissue. For the cylinder phantom, as shown in Figure 1(a), two cylinders are used to simulate the soft tissue. The phantom shown in Figure 1(e) uses two ellipses to simulate the soft tissue and is referred to as ellipse phantom. The density of soft tissue is approximated with the density of water. The shapes are placed such that they appear as close as possible to real knees.

In a next step, the phantoms are forward projected to the sinogram domain. During that step, a synthetic overexposure simulation is performed as follows: From each view the histogram is computed and all values that are beyond a pre-defined range are set to zero in the sinogram.

Using these overexposed sinograms, a state of the art and the proposed algorithms are applied. The ground truth is obtained using the filtered backprojection of the non-overexposed knee phantom. A quantitative comparison is performed using the root mean square error (RMSE) and relative root mean square error (rRMSE) with respect to the ground truth. We also investigated the performance of the standard water cylinder extrapolation [1] and compare it with our proposed method. At the position of discontinuity, i.e. the truncation edge, the projection of a water cylinder is fitted. The position and size of the fitted cylinder can be computed by fulfilling the continuity assumption of the truncation edge. In a second step, with the mass consistency the cylinders are adjusted so that the resulting extrapolated mass per view, is equal to the real/reference mass. In our algorithm, this is done by adjusting the slope, followed by a cosine-smoothing.

For the optimization approach, the first step is to initialize the cylinder parameters. By heuristics, we use two cylinders to estimate the thigh bones, two cylinders for the soft tissues and six cylinders for the patellas. That results in a total of ten cylinders and 40 parameters. The initial parameters are approximated empirically as follows: The greatest value of the whole sinogram is expected to be the ray, where both knee bones overlap most. In an orthogonal view, the two highest values are expected to mark the position of the two thigh bones. By finding the intersection of these rays, the centers of the two knees are approximated. Then the radius of the soft tissue is approximated with the slope and intensity value at the edges in the orthogonal view. In practice, the initial parameters can be computed by using an initial reconstruction and extracting the parameters from the overexposed image. After optimization, the areas where real data is missing due to overexposure are completed by the values that are extrapolated using the fitted shapes.

3 Results

The reconstruction results of the proposed method, compared with the reference, method without correction and the water cylinder extrapolation, are presented in Figure 1. Both correction algorithms increase the image quality with respect to no correction, cf. Figure 1(b) and 1(f). The water cylinder approach shown in Figure 1(c) and 1(g) removes artifacts in the center-lateral direction but the up-

Correction Model	Phantom	RMSE	rRMSE	Improvement
Water Cylinder Extrapolation	Cylinder	0.1342	0.1119	66 %
Optimization with Cylinders	Cylinder	0.0300	0.0250	92 %
No Correction	Cylinder	0.3899	0.3249	0 %
Water Cylinder Extrapolation	Ellipse	0.1581	0.1318	66 %
Optimization with Cylinders	Ellipse	0.1643	0.1388	64 %
No Correction	Ellipse	0.4680	0.3900	0 %

Table 1. Table of the RMSE, rRMSE and Improvement for the optimization approach, the water cylinder extrapolation and no correction applied on the cylinder- and ellipse phantom.

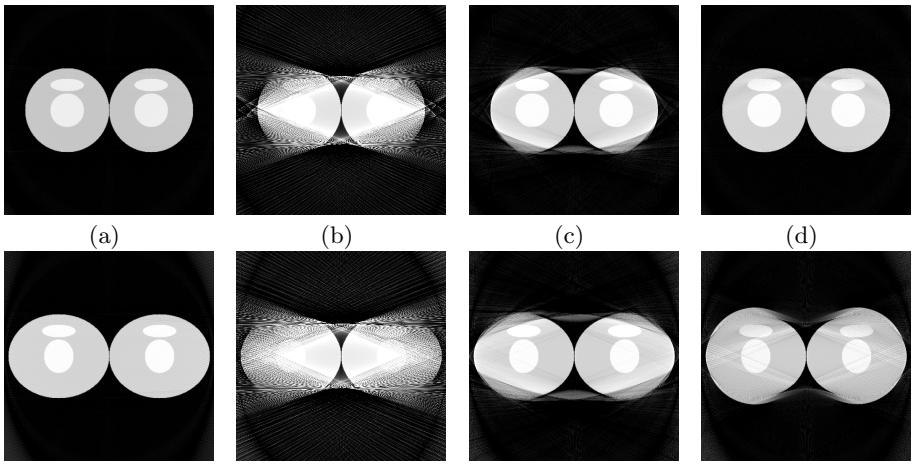

Fig. 1. Reconstructions for the cylinder and the ellipse phantom in the top and bottom row, respectively. From left to right: Ground truth, overexposed reconstructions without correction, the corrected reconstruction using mass constrained water cylinder extrapolation and the reconstructions of the proposed optimization-based approach. The visualization window was set to [0, 1.2].

per and lower boarders of the knee still suffer from artifacts. With the optimization approach, the cylinder phantom can be reconstructed close to the ground truth, as shown in Figure 1(d). Applied to the ellipse phantom, the streaking artifacts are removed but the original contour is not recovered. However within 1(d) and 1(h) the shape of the patella is reconstructed close to the ground truth.

The quantitative results are presented in Table 1. With both methods the RMSE and rRMSE are substantially lower compared to no correction. The cylinder optimization reduces the error by 92 % within the cylinder phantom, whereas the water cylinder extrapolation reduces the error by 66 %. The ability of the optimization to improve the image lowers when applied to the ellipse phantom.

The improvement of the water cylinder extrapolation remains unchanged at 66 % when applied on the ellipse phantom.

4 Discussion

Both extrapolation approaches recover the central-lateral regions close to the ground truth. In these directions, the knees do not overlap in the projections and the extrapolation performed by the water cylinder correction is very precise. In the areas where the knees overlap, this algorithm cannot provide exact reconstructions. The extrapolation scheme consists of local continuity condition at the truncation edges and has not enough information to extrapolate more then one cylinder close to the ground truth. That information is provided by the optimization approach, which is thus capable to extrapolate a composite of cylinders. The only areas that differ from the ground truth, are the patella regions, where the transitions are blurred. The optimization approach faces challenges, when it comes to shapes that can not be modeled with cylinders. The fitted shape is either to small or to great to simulate the real object.

This may be handled when introducing more complex geometric shapes like ellipses, splines or level-sets. A further improvement to the proposed algorithm is increasing the number of fitted independent shapes. The future work involves the validation of the proposed method using real knee data.

References

1. Hsieh J, Chao E, Thibault J, Grekowicz B, Horst A, McOlash S, et al. A novel reconstruction algorithm to extend the CT scan field-of-view. Medical Physics. 2004;31(9):2385–2391.
2. Ohnesorge B, Flohr T, Schwarz K. Efficient correction for CT image artifacts caused by objects extending outside the scan field of view. Medical Physics. 2000;27(1):39–46.
3. Ritschl L, Knaup M, Kachelrieß M. Extending the dynamic range of flat detectors in CBCT using a compressed-sensing-based mulit-exposure technique. In: The 12th International Meeting on Fully Three-Dimensional Image Reconstruction in Radiology and Nueclear Medicine - Proceedings; 2013. p. 26–29.
4. Van Gompel G, Defrise M, Van Dyck D. Elliptical extrapolation of truncated 2D CT projections using Helgason-Ludwig consistency conditions. Proc SPIE. 2006;6142:61424B–61424B–10.
5. Dennerlein F, Maier A. Region-of-interest reconstruction on medical C-arms with the ATRACT algorithm. In: Pelc NJ, Nishikawa RM, Whiting BR, editors. SPIE Medical Imaging; 2012. p. 83131B–83131B–9.
6. Xia Y, Hofmann H, Dennerlein F, Mueller K, Schwemmer C, Bauer S, et al. Towards Clinical Application of a Laplace Operator-Based Region of Interest Reconstruction Algorithm in C-Arm CT. Medical Imaging, IEEE Transactions on. 2014 March;33(3):593–606.
7. Maier A, Scholz B, Dennerlein F. Optimization-based Extrapolation for Truncation Correction. Salt Lake City, Utah, USA; 2012. p. 390–394.